Rotationally resolved energy-dispersive photoelectron spectroscopy of H 2 O: Photoionization of the C̃ (0,0,0) state at 355 nm

W. L. Glab, P. T. Glynn, P. M. Dehmer, J. L. Dehmer, Kwanghsi Wang, and B. V. McKoy

Citation: The Journal of Chemical Physics **106**, 5779 (1997); doi: 10.1063/1.473597
View online: http://dx.doi.org/10.1063/1.473597
View Table of Contents: http://scitation.aip.org/content/aip/journal/jcp/106/13?ver=pdfcov
Published by the AIP Publishing

Rotationally resolved energy-dispersive photoelectron spectroscopy of H_2O: Photoionization of the $\tilde{C}(0,0,0)$ state at 355 nm

W. L. Glab and P. T. Glynn
Department of Physics, Department of Physics, Texas Tech University, P.O. Box 41051, Lubbock, Texas 79409

P. M. Dehmer[a] and J. L. Dehmer[b]
Argonne National Laboratory, Argonne, Illinois 60439

Kwanghsi Wang and B. V. McKoy
Noyes Laboratory of Physical Chemistry, California Institute of Technology, Pasadena, California 91125

(Received 20 September 1996; accepted 27 January 1997)

Measured and calculated rotationally resolved photoelectron spectra for photoionization of low rotational levels of the $\tilde{C}\ ^1B_1$ Rydberg state of water are reported. This is the first example of rotationally resolved photoionization spectra beyond the special cases of H_2, high-J levels, and threshold spectra. These spectra reveal very nonatomiclike behavior and, surprisingly, the influence of multiple Cooper minima in the photoelectron matrix elements. © *1997 American Institute of Physics.* [S0021-9606(97)02713-X]

High-resolution, energy-dispersive photoelectron spectroscopy (PES) has been an important experimental probe of photoionization processes in atomic and molecular systems. Such photoelectron analyzers have been used to obtain rotationally resolved spectra for light systems such as H_2 (Ref. 1) and for high J levels of heavier diatomics such as NO (Ref. 2) and OH (Ref. 3), thus permitting detailed comparisons between theoretical predictions and experimental observations. These studies have highlighted important dynamical features such as angular momentum mixing in the molecular electronic continuum, parity selection rules, and the effects of Cooper minima on photoelectron spectra.[4,5] While zero-kinetic-energy (ZEKE) photoelectron spectroscopy[6] can provide subwavenumber resolution in ion rotational distributions, this technique is restricted to the threshold region and does not permit studies at photoelectron energies away from the threshold. Studies at higher photoelectron energies can clearly display dynamical behavior which may not be apparent from near-threshold studies. This is particularly true of features arising from Cooper minima.

In this Communication we present the first rotationally resolved, REMPI (resonance enhanced multiphoton ionization) photoelectron spectra for low rotational levels of any molecule other than H_2 at energies significantly above threshold. Spectra were measured for $(2+1')$ REMPI of selected rotational levels of the $\tilde{C}\ ^1B_1(0,0,0)$ state of H_2O at about 1 eV above threshold with a kinetic energy resolution of about 4 meV. Comparison of these experimental results with calculated ion yield distribution reveals both very nonatomiclike photoionization dynamics and the influence of multiple Cooper minima in the photoelectron channels.

Room temperature water vapor at a pressure of $\sim 2\times10^{-5}$ Torr was photoionized through a $(2+1')$ process, resonant at the two-photon level with selected rotational levels of the $\tilde{C}$ vibrational state. The tunable light used to excite the $\tilde{C}\ ^1B_1(0,0,0)$ state was produced by frequency doubling the tunable 490 nm light from a homebuilt dye laser/amplifier (band-width $\sim 0.03\ \mathrm{cm}^{-1}$), yielding up to 200 μJ of ultraviolet light. The dye laser was pumped by the third-harmonic output of a Nd^{+3}:YAG laser (Continuum YG661) operating at a 10 Hz repetition rate, with a pulse duration of about 6 ns. An autotracking device (INRAD AT-2) was used to maintain optimum ultraviolet intensity when the laser wavelength was scanned. The ultraviolet light was separated from the visible fundamental using dichroic mirrors and was focused into the electron spectrometer using a 7.5 cm focal length lens. Wavelength scans were calibrated using a simultaneously acquired optogalvanic reference spectrum of uranium. Typically, 5 mJ of 355 nm light was used to photoionize the $\tilde{C}$ state. This light was obtained from the third-harmonic beam of the Nd^{+3}:YAG laser and was directed to the magnetic bottle photoelectron spectrometer and focused into the interaction region using a 20-cm focal length lens. This photoionizing radiation, which was polarized parallel to the magnetic field in the photoelectron spectrometer, was counterpropagated with the 245 nm light from the doubled dye laser. A high energy density of photoionizing radiation was required to compete effectively with predissociation of the $\tilde{C}$ state.[7]

The magnetic bottle photoelectron spectrometer, which will be described in detail elsewhere,[8] is a modified version of the instrument described in Ref. 9. Briefly, the photoionization process occurs in a uniform 1 T magnetic field which is produced by an electromagnet. Photoelectrons spiral out from the interaction region along the field direction and travel through a hole in one of the pole faces into a drift tube. The drift tube has a uniform 10^{-3} T field directed along its axis, produced by a solenoidal coil. The magnetic field in the

[a]Current address: U.S. Department of Energy, Office of Basic Energy Sciences, ER-10, Germantown, Maryland 20874-1290.
[b]Current address: Optical Technology Division, National Institute of Standards and Technology, Gaithersburg, Maryland 20899.

transition region, determined by the shape of the pole faces, decreases smoothly from one field value to the other. Electrons with an initial velocity component in the direction of the drift tube and sufficiently low energy pass adiabatically (without crossing field lines) from the interaction region into the drift tube region and thus have their paths redirected towards the detector without a change in their kinetic energies. The collection efficiency of the spectrometer is therefore roughly 50%. The drift tube can be biased with a retarding voltage to spread out the arrival time of the electrons at the detector for the kinetic energy range of interest. The photoelectrons are detected with a tandem microchannel plate. The detector signal for each laser shot is processed by a transient digitizer and stored on a computer. A typical photoelectron time-of-flight spectrum is acquired by averaging the data for 5000 laser shots. Tests of this spectrometer on $(3+1')$ photoionization of krypton have demonstrated a resolution of 3.5 meV for 1 eV photoelectrons.

Accurate calibration of time-of-flight instruments such as the one used in this experiment is difficult; however, if the full photoelectron spectrum contains several peaks with known energies that do not differ greatly from those of the peaks of interest, the spectrum may be calibrated accurately by a fit of the known energies to the arrival times. This procedure will be discussed in more detail in a subsequent paper.[7] In the case of this experiment, three known peaks are provided by nonresonant four-photon ionization of the lowest three vibrational states of the ground state by the 355 nm light. Using these peaks, we were able to calibrate the absolute energies of the remaining peaks in the spectra to an accuracy of about 2 meV. The accuracy of the relative energy spacings within the photoelectron spectra should be significantly better than 1 meV.

In this work, we also present the results of *ab initio* calculations of the rotationally resolved photoelectron spectrum for photoionization of the $\tilde{C}\ ^1B_1(3pa_1)$ Rydberg state leading to the $\tilde{X}\ ^2B_1$ ground state of H_2O^+. The wave function of the $\tilde{C}$ state is obtained using the improved virtual orbital (IVO) method,[10] and the core orbitals are taken to be those of the fully relaxed core of the ion. For the final state, we used the frozen-core Hartree–Fock approximation, in which the photoelectron orbital is obtained as a solution of a one-electron Schrödinger equation containing the Hartree–Fock potential of the molecular ion. The photoelectron orbitals are obtained numerically using an iterative procedure to solve the associated Lippmann–Schwinger equation.[11,12] These calculations emphasize the importance of the nonspherical nature of the molecular ion potential and the formation of the Cooper minima in the electronic continuum.

In these calculations, the molecular z axis is chosen to be the C_2 symmetry axis and the x axis is in the plane of the molecule (or ion). Thus, the body-fixed axes x, y, and z coincide with the a, c, and b axes, respectively. With this choice and using Hund's case b to represent the $\tilde{C}$ Rydberg and $\tilde{X}$ ionic states of water, the dipole transition matrix element can be written as

$$\langle f|\mu|i\rangle = \sum C[1+(-1)^{\Delta N+\Delta p+l+1}] \begin{pmatrix} N_t & 1 & l \\ -K_t & \mu & \lambda \end{pmatrix} \times \left[\begin{pmatrix} N_+ & N_i & N_t \\ -K_+ & K_i & K_t \end{pmatrix} + (-1)^{p_+} \begin{pmatrix} N_+ & N_i & N_t \\ K_+ & K_i & K_t \end{pmatrix} \right], \tag{1}$$

with $\Delta N = N_+ - N_i$ and $\Delta p = p_+ - p_i$. In Eq. (1), C is related to the electronic transition dipole moment,[13] N_+ and N_i are the total angular momenta (exclusive of spin) for the ion and Rydberg state of H_2O, respectively, K_+ and K_i are their projections on the z axis, and p_+ and p_i are the parities of their rotational wave functions. N_t denotes the angular momentum transfer, l an angular momentum component of the photoelectron matrix element, λ its projection along the molecular z axis, and μ the light polarization index in the molecular frame.

With the symmetry properties of the asymmetric top and our choice of the molecular axes, it can be shown that ΔK_a is even (odd) when $\Delta N + \Delta p$ is even (odd). Using this relationship and Eq. (1), we obtain the selection rule

$$\Delta K_a + l = \text{odd}, \tag{2}$$

and

$$\Delta K_b = \mu + \lambda, \tag{3}$$

with $\Delta K_a = K_a^+ - K_a^i$ and $\Delta K_b = K_b^+ - K_b^i$, where K_a and K_b are the projections of the total angular momentum (except spin) along the a and b axes, respectively. To obtain the selection rules for photoionization of the $\tilde{C}\ ^1B_1(3pa_1)$ Rydberg state of H_2O, we have to determine the value of $\mu+\lambda$. There are three dipole-allowed continuum channels kb_2, kb_1, and ka_1 for this ionization process. In this case, odd λ and μ are associated with the kb_1 and kb_2 channels, whereas even λ and μ are associated with the ka_1 channel. Therefore, $\lambda+\mu$ is always even for all allowed transitions. Hence we have

$$\Delta K_a + \Delta K_c = \text{even}. \tag{4}$$

Equations (2) and (4) show that only type b transitions are allowed. Those transitions with ΔK_a=odd and ΔK_c=odd are associated with even l partial waves of the photoelectron matrix elements and those with ΔK_a=even and ΔK_c=even with odd l partial waves.

Figure 1 shows the total photoelectron signal from the $(2+1')$ ionization process vs transition energy over part of the $\tilde{C} \leftarrow\leftarrow \tilde{X}$ band, acquired by scanning the wavelength of the dye laser. The transitions to the red of the bandhead at $\sim$80670 cm^{-1} have been observed previously by $(2+1)$ ionization and identified, as described in Ref. 14. Our measured transition energies differ from those of Ref. 14 by at most 0.2 cm^{-1}. Most of the peaks to the red of the bandhead are well-resolved; therefore, we were able to excite these selectively and acquire photoelectron spectra corresponding to a pure or nearly pure population of individual rotational levels of the $\tilde{C}$ state. In this communication, we report rotationally

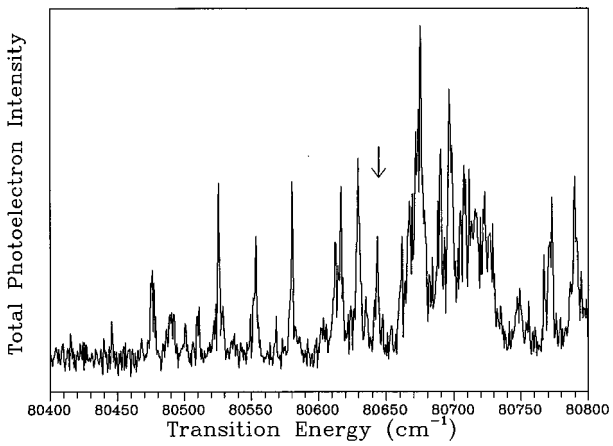

FIG. 1. A portion of the $(2+1')$ photoionization spectrum of the $\tilde{C}(0,0,0)\leftarrow\leftarrow\tilde{X}(0,0,0)$ transition. The arrow indicates the transition: $4_{13}\leftarrow\leftarrow 4_{14}$.

resolved photoelectron spectra for the rotational level 4_{13}, excited from the 4_{14} level of the ground state as indicated by the arrow in Fig. 1.

Figure 2 shows our calculated rotationally resolved photoelectron spectra along with the measured $(2+1')$ REMPI spectra for photoionization of the 4_{13} rotational level of the $\tilde{C}\ ^1B_1(3pa_1)$ Rydberg state of H_2O leading to the $\tilde{X}\ ^2B_1$ state of H_2O^+. The calculated spectrum is convoluted with a Gaussian detection function having a full width at half maximum of 42 cm^{-1}. Agreement between the calculated and measured spectra is very encouraging. These spectra show only type b transitions [ΔK_a=even(odd), ΔK_c=even(odd)] with the most intense transition being $4_{13}\leftarrow 4_{13}$. On the basis of the selection rules of Eqs. (2) and (4), this transition must arise from odd partial waves of the photoelectron matrix element. Single-center expansion of the $3pa_1$ orbital reveals that it has 14.54% s, 83.55% p, and 1.89% d character. In view of this strong odd wave character of the $3pa_1$ orbital, this intense $4_{13}\leftarrow 4_{13}$ peak in the photoelectron spectrum must be very molecular in origin and arise from strong l-mixing in the molecular electronic continuum. Similar behavior is also clearly seen in the mixed peak for the 5_{33} and 6_{15} ionic levels. While the other ΔK_a=even and ΔK_c=even (l=odd) transitions such as 3_{31}, 5_{15}, and 4_{31} levels are also dominant, they are mixed with other rotational peaks arising from even l components of the photoelectron matrix element.

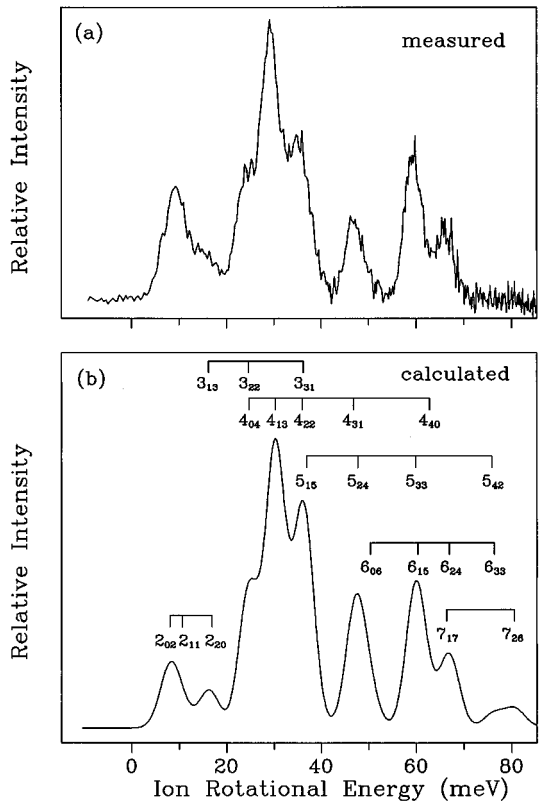

FIG. 2. (a) measured and (b) calculated rotationally resolved photoelectron spectra for photoionization of the 4_{13} rotational level of the $\tilde{C}\ ^1B_1(0,0,0)$ state of water.

To provide some insight into the dynamical aspects of the angular momentum transfer of the photoelectron upon ionization in this system, we closely examined the photoelectron matrix elements for the electron kinetic energies up to 10 eV. Surprisingly, multiple Cooper minima are seen in every continuum channel around 2 eV. For example, these minima exist in the d and f waves of the ka_1 channel, p, d, f, and g waves of the kb_1 channel, and the f and g waves of the kb_2 channel.[15] These Cooper minima strongly deplete the contributions of the even and odd waves around 2 eV. The photoelectron energies in our experiment are around 0.87 eV. At this energy, the contributions of the odd (especially p and f) waves are much stronger than those of even waves. Strong partial-wave mixing near threshold is also clearly seen; this behavior is quite common for systems with large dipole moments. Further studies on this system are underway to study the influence of these Cooper minima on ion rotational distributions at energies around 2 eV.

The work at California Institute of Technology was supported by grants from the Air Force Office of Scientific Research and the Office of Health and Environmental Research of the U.S. Department of Energy. We also acknowledge use of the resources of the Jet Propulsion Laboratory/California Institute of Technology CRAY Y-MP2E/116 Supercomputer. The authors wish to acknowledge useful discussions with Dr. S. T. Pratt. The photoelectron spectrometer at Argonne National Laboratory had been constructed with support from the Office of Health and Environmental Research of the U.S. Department of Energy. W.L. Glab and P.T. Glynn were partially supported by the Robert A. Welch Foundation.

[1] S. L. Anderson, G. D. Kubiak, and R. N. Zare, Chem. Phys. Lett. **105**, 22 (1984).
[2] K. S. Viswanathan, E. Sekreta, and J. P. Reilly, J. Phys. Chem. **90**, 5658 (1986).
[3] E. de Beer, C. A. de Lange, J. A. Stephens, K. Wang, and V. McKoy, J. Chem. Phys. **95**, 714 (1991).
[4] See the review article, S.T. Pratt, Rep. Prog. Phys. **58**, 821 (1995).
[5] K. Wang and V. McKoy, Annu. Rev. Phys. Chem. **46**, 275 (1995).

[6] K. Müller-Dethlefs and E. W. Schlag, Annu. Rev. Phys. Chem. **42**, 109 (1991).
[7] M. N. R. Ashfold, J. M. Bayley, and R. N. Dixon, Chem. Phys. **84**, 35 (1984).
[8] W. I. Glab, P. M. Dehmer, and J. L.Dehmer (in preparation).
[9] P. Kruit and F. H. Read, J. Phys. E **16**, 313 (1983).
[10] W. J. Hunt and W. A. Goddard, Chem. Phys. Lett. **3**, 414 (1969).
[11] R. R. Lucchese, G. Raseev, and V. McKoy, Phys. Rev. A **25**, 2572 (1982).
[12] M. Braunstein, V. McKoy, L. E. Machado, L. M. Brescansin, and M. A. P. Lima, J. Chem. Phys. **89**, 2998 (1988).
[13] M.-T. Lee, K. Wang, V. McKoy, and L. E. Machado, J. Chem. Phys. **97**, 3905 (1992).
[14] G. Meijer, J. J. ter Meulen, P.Andresen, and A. Bath, J. Chem. Phys. **85**, 6914 (1986).
[15] W. L. Glab, P. T. Glynn, P. M. Dehmer, J. L. Dehmer, K. Wang, and V. McKoy (in preparation).